Acta Crystallographica Section B
Structural Science
ISSN 0108-7681

Three isomeric 1-(2-chloronicotinoyl)-2-(nitrophenyl)hydrazines, including three polymorphs of 1-(2-chloronicotinoyl)-2-(2-nitrophenyl)hydrazine: hydrogen-bonded supramolecular structures in two and three dimensions

Solange M. S. V. Wardell,[a] Marcus V. N. de Souza,[a] James L. Wardell,[b] John N. Low[c] and Christopher Glidewell[d]*

[a]Fundação Oswaldo Cruz, Far Manguinhos, Rua Sizenando Nabuco, 100 Manguinhos, 21041-250 Rio de Janeiro-RJ, Brazil, [b]Instituto de Química, Departamento de Química Inorgânica, Universidade Federal do Rio de Janeiro, CP 68563, 21945-970 Rio de Janeiro-RJ, Brazil, [c]Department of Chemistry, University of Aberdeen, Meston Walk, Old Aberdeen AB24 3UE, Scotland, and [d]School of Chemistry, University of St Andrews, St Andrews, Fife KY16 9ST, Scotland

Correspondence e-mail: cg@st-andrews.ac.uk

Received 12 April 2006
Accepted 12 October 2006

1-(2-Chloronicotinoyl)-2-(2-nitrophenyl)hydrazine, $C_{12}H_9ClN_4O_3$, crystallizes in three polymorphic forms, two monoclinic forms in space groups *Cc* (I*a*) and $P2_1$ (I*b*), and an orthorhombic form in space group *Pbcn* (I*c*). In the *Cc* polymorph (I*a*) the molecules are linked into sheets by combinations of one N—H···O and two C—H···O hydrogen bonds, while in the $P2_1$ polymorph (I*b*) the molecules are linked into sheets by combinations of three hydrogen bonds, one each of N—H···O, C—H···N and C—H···O types. In the orthorhombic polymorph (I*c*) the molecules are linked into a complex three-dimensional framework structure by a combination of one N—H···O, one N—H···N and three C—H···O hydrogen bonds, and an aromatic $\pi\cdots\pi$ stacking interaction. In the isomeric compound 1-(2-chloronicotinoyl)-2-(3-nitrophenyl)hydrazine (II) the molecules are again linked into a three-dimensional framework, this time by a combination of three hydrogen bonds, one each of N—H···O, N—H···N and C—H···O types, weakly augmented by a $\pi\cdots\pi$ stacking interaction. The molecules of 1-(2-chloronicotinoyl)-2-(4-nitrophenyl)hydrazine (III) are linked into sheets by a combination of three hydrogen bonds, one each of N—H···O, N—H···N and C—H···O types.

1. Introduction

Here we report the molecular and supramolecular structures of three isomeric 1-(2-chloronicotinoyl)-2-(nitrophenyl)hydrazines, (I)–(III), whose molecular constitutions differ only in the location of the nitro group within the nitrophenyl ring (see scheme below); in addition, compound (I), 1-(2-chloronicotinoyl)-2-(2-nitrophenyl)hydrazine, has been identified in

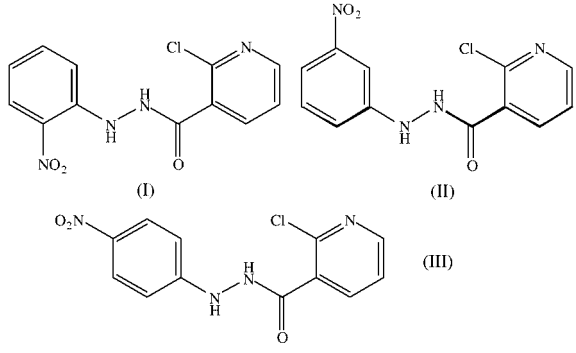

three polymorphic forms, denoted (I*a*), (I*b*) and (I*c*), crystallizing in space groups *Cc*, $P2_1$ and *Pbcn*, respectively.

This work is a direct extension of our recent studies on the analogous isomeric 2-chloro-*N*-(nitrophenyl)nicotinamides

(IV)–(VI) (de Souza *et al.*, 2005) and on a series of 4-substituted *N*-aryl-2-chloronicotinamides (VII) (Cuffini *et al.*, 2006), and it describes significant changes in hydrogen bonding, and hence in the overall supramolecular structures, in a series of three geometric isomers, one of which occurs in three polymorphic forms.

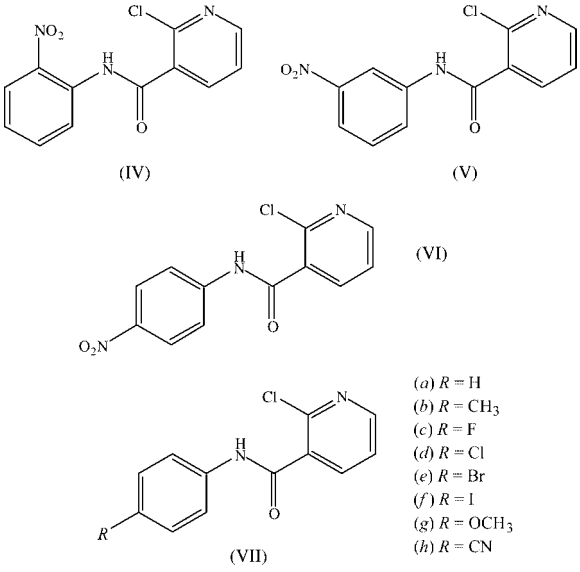

The three nitro-substituted amides (IV)–(VI) differ only in the location of a single substituent. However, they exhibit crystallization characteristics, where isomer (IV) crystallizes in anhydrous form with $Z' = 1$, isomer (V) crystallizes as a monohydrate and isomer (VI) crystallizes in anhydrous form with $Z' = 2$. In addition, they also differ in their conformations, in the identity of the direction-specific intermolecular forces manifested and hence in their overall supramolecular aggregation. Of the two unsolvated isomers in this series, the molecules of isomer (IV) are linked into chains of edge-fused rings by two independent C—H···O hydrogen bonds, whereas those of isomer (VI) are linked into simple chains by two independent N—H···N hydrogen bonds: N—H···N hydrogen bonds are absent from the structure of isomer (IV) and C—H···O hydrogen bonds are absent from the structure of isomer (VI). In the hydrated structure of compound (V), the molecular components are again linked into a chain of edge-fused rings, but with different ring motifs from those in (IV). Three types of hydrogen bond, N—H···O, O—H···O and O—H···N, are present in the structure of (V), but C—H···O and N—H···N hydrogen bonds, as found in isomers (IV) and (VI), respectively, are absent from the structure of (V).

In series (VII), where the molecular variation takes the form of altering the substituent at a constant location, position 4, in the aryl ring, as opposed to the different locations of a common substituent in the isomeric series (IV)–(VI), again each compound exhibits a different range of direction-specific intermolecular forces, leading to a very wide range of supramolecular structures in one, two or three dimensions. In addition, none of the pairs which might reasonably have been expected to be isostructural, such as (VII*b*) and (VII*d*), (VII*d*) and (VII*e*), or (VII*e*) and (VIII*f*), are in fact even approximately isostructural: these four compounds (VII*b*, VII*c*, VII*d*, VII*e*, VII*f*) crystallize, respectively, in space groups $P\overline{1}$ with $Z' = 2$, $P2_1$ with $Z' = 4$, $P2_12_12_1$ with $Z' = 1$, and $Pbca$ with $Z' = 1$. In addition, we also note the bis(nicotinoyl) derivative (VIII), obtained as a by-product in the synthesis of compound (V) (Wardell, Wardell *et al.*, 2006): this crystallizes as a monohydrate, and the components are linked into sheets by no fewer than five independent hydrogen bonds.

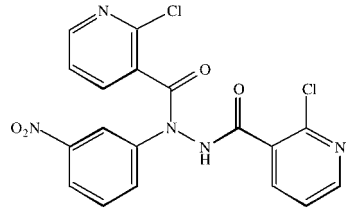

In view of the very wide variation in supramolecular structures engendered by rather modest changes in molecular constitution in (IV)–(VI), or molecular composition in series (VII), we have now investigated the isomeric hydrazines (I)–(III). These compounds are closely related to the amides (IV)–(VI), but the presence of a further angular component in the spacer unit between the two rings not only introduces a further potential donor and acceptor of hydrogen bonds but subtly alters the relative orientation, as compared with the amide analogues, of several of the other acceptor sites, in particular the pyridyl N and the nitro O atoms. The two series (I)–(III) and (IV)–(VI) form part of a continuing study of the variations in supramolecular structures of extended series of isomeric compounds (Ferguson *et al.*, 2005; Glidewell *et al.*, 2002, 2005, 2006; Kelly *et al.*, 2002; Wardell *et al.*, 2002; Wardell, Low *et al.*, 2006).

We discuss below the supramolecular structures of compounds (I)–(III) in order of increasing complexity, and the polymorphs are labelled in accordance with this. Polymorph (I*b*) was strictly the first form to be isolated, as it crystallized directly from the solution in which compound (I) had been synthesized. However, because the crystals of (I*b*) were of rather poor quality, illustrated for example by the $R_{\rm int}$ value of 0.178 and the final R value of 0.0739, crystallizations were undertaken from two other solvents, leading to the identification of the *Cc* polymorph denoted (I*a*) and the *Pbcn* polymorph denoted (I*c*). By contrast, the same form for isomer (III) was obtained whether it was crystallized from methanol, ethanol or acetone.

2. Experimental

2.1. Synthesis

For the synthesis of compound (I), a solution of 2-chloronicotinoyl chloride (3 mmol) and 2-nitrophenylhydrazine (3 mmol) in 1,2-dichloroethane (30 cm^3) was boiled under reflux for 30 min. On cooling, crystals of the $P2_1$ polymorph (I*b*) (m.p. 418–420 K) were deposited, which proved to be just adequate for single-crystal X-ray diffraction. Evaporation of

the mother liquor under reduced pressure left a solid residue, which on crystallization from ethanol gave the *Cc* polymorph (I*a*), while crystallization from acetone gave the orthorhombic polymorph (I*c*), both suitable for single-crystal X-ray diffraction: for (I*a*), the crystals were fragile, and attempts to cut small fragments from larger crystals repeatedly led to the shattering of the crystals. MS: *m*/*z* 292 $[M]^+$. NMR (DMSO-d_6) δ(H): 6.93 (1H, dd, *J* = 7.28 and 8.13 Hz, H5′), 7.33 (1H, d, *J* = 7.98 Hz, H6′), 7.60 (1H, dd, *J* = 4.83 and 7.52 Hz, H5), 7.67 (1H, ddd, *J* = 1.29, 8.45 and 7.16 Hz, H4′), 8.10 (1H, dd, *J* = 1.84 and 7.53 Hz, H4), 8.14 (1H, dd, *J* = 1.20 and 8.48 Hz, H3′), 8.56 (1H, dd, *J* = 1.82 and 4.79 Hz, H6), 9.43 (1H, s, NH), 10.94 (1H, s, NH); δ(C) 114.8, 118.2, 123.2, 125.9, 130.9, 132.0, 136.6, 138.8, 144.8, 146.8, 151.1, 164.8. IR (cm^{-1} KBr pellet) 3268 (NH), 1684 (CO).

For the synthesis of compound (II), a solution of 2-chloronicotinoyl chloride (3 mmol) and 3-nitrophenylhydrazine hydrochloride (3 mmol) in 1,2-dichloroethane (60 cm^3) was boiled under reflux for 30 min. The mixture was cooled and the solvent was removed under reduced pressure. Crystals suitable for single-crystal X-ray diffraction were grown by slow evaporation of a solution in 1,2-dichloroethane/ethanol (1:1 *v*:*v*), m.p. 414–414 K. MS: *m*/*z* 292 $[M]^+$. NMR (DMSO-d_6) δ(H): 7.28 (1H, dd, *J* = 1.48 and 7.0 Hz, H6′), 7.48 (1H, dd, *J* = 8.12 and 8.09 Hz, H5′), 7.58 (1H, dd, *J* = 5.08 and 7.58 Hz, H5), 7.60 (1H, dd, *J* = 8.18 and 1.29 Hz, H4′), 7.69 (1H, dd, *J* = 2.05 and 2.12 Hz, H2′), 8.06 (1H, dd, *J* = 1.89 and 7.52 Hz, H4), 8.56 (1H, dd, *J* = 1.89 and 4.83 Hz, H6), 8.76 (1H, s, NH), 10.61 (1H, s, NH); δ(C) 105.9, 113.2, 118.6, 123.2, 130.2, 131.2, 138.5, 146.7, 148.7, 150.1, 150.9, 165.1. IR (cm^{-1} KBr pellet) 3270 (NH), 1693 (CO).

For the synthesis of compound (III), a solution of 2-chloronicotinoyl chloride (3 mmol) and 4-nitrophenylhydrazine (3 mmol) in 1,2-dichloroethane (60 cm^3) was boiled under reflux for 30 min. The mixture was cooled and the solvent was removed under reduced pressure. Crystals suitable for single-crystal X-ray diffraction were grown by slow evaporation of a solution in acetone, m.p. 500–502 K decomposes with gas evolution and the formation of a brown solid. Samples crystallized from methanol and ethanol gave the same crystal form as crystallization from acetone. NMR (DMSO-d_6) δ(H): 6.93 (2H, d, *J* = 8.5 Hz), 7.59 (1H, dd, *J* = 6.5 and 5.0 Hz), 8.11–8.13 (3H, m), 8.57 (1H, dd, 4.5 and 1.5 Hz), 9.38 (1H, s, NH), 10.72 (1H, s, NH); δ(C) 110.8, 123.1, 125.8, 130.9, 138.3, 138.6, 146.7, 151.0, 154.3, 164.8. IR (cm^{-1} KBr pellet) 3256 (NH), 1673 (CO).

2.2. Data collection, structure solution and refinement

Details of cell data, data collection and structure solution and refinement are summarized in Table 1 (Ferguson, 1999; Hooft, 1999; McArdle, 2003; Otwinowski & Minor, 1997; Sheldrick, 1997, 2003). For each of (I*a*) and (III), the systematic absences permitted *Cc* and *C*2/*c* as possible space groups: in view of the unit-cell volumes, *Cc* was selected for each, and in both cases this choice was confirmed by the successful structure analysis. Careful searches for possible addition symmetry revealed none. For (I*b*), the systematic absences permitted $P2_1$ and $P2_1/m$ as possible space groups: $P2_1$ was selected and confirmed by the successful structure analysis. For (I*c*) and (II), the space groups *Pbcn* and $P2_1/c$, respectively, were uniquely assigned from the systematic absences. The structures were all solved by direct methods using *SHELXS*97 (Sheldrick, 1997), and refined on F^2 with all data using *SHELXL*97 (Sheldrick, 1997). A weighting scheme based upon $P = (F_o^2 + 2F_c^2)/3$ was employed in order to reduce statistical bias (Wilson, 1976). All H atoms were located in difference maps and then treated as riding atoms; H atoms bonded to C atoms had distances of 0.95 Å and $U_{iso}(H) = 1.2U_{eq}(C)$; H atoms bonded to N atoms were permitted to ride at the N—H distances deduced from the difference maps, 0.83–0.94 Å, and with $U_{iso}(H) = 1.2U_{eq}(N)$. For (I*b*) the absolute configuration of the molecules in the crystal selected for data collection was established by means of the Flack parameter (Flack, 1983), although this configuration has no chemical significance; for each of (I*a*) and (III), the correct orientation of the structure with respect to the polar axis directions was established by means of the Flack parameter (Table 1).

Supramolecular analyses were made, and the diagrams were prepared with the aid of *PLATON* (Spek, 2003). Fig. 1 shows the independent components of compounds (I)–(V) with the atom-labelling schemes and Figs. 2–7 show aspects of their supramolecular structures. Selected torsional angles are given in Table 2 and details of the hydrogen bonding are in Table 3.[1]

3. Results and discussion

3.1. Crystallization characteristics

Of the five independent structures reported here, we note that three of these, (I*a*), (I*b*) and (III), crystallize in non-centrosymmetric space groups: in particular (I*a*) and (III) both crystallize in space group *Cc*. The perils of space group *Cc* have been fully documented (Baur & Kassner, 1992; Marsh, 1997, 2004), and it remains the case (Marsh, 2004) that for structures being deposited in the Cambridge Structural Database (CSD; Allen, 2002) around 10% of those reported to be in space group *Cc* continue to suffer from an error in the assignment of the space group. Hence to find two examples of space group *Cc* in a sample of five related structures immediately causes concern. However, not only does the *ADDSYM* routine in *PLATON* (Spek, 2003) find no additional symmetry in either (I*a*) or (III), but each crystallizes with *Z* = 4, and in a conformation such that the molecule does not have even approximate internal symmetry; in addition, the molecular constitutions rule out any possibility that the molecules could lie across either rotation axes or centres of inversion, except in the presence of serious disorder, for which no evidence was found. Hence we conclude that the space-group assignments for (I*a*) and (III) are correct.

[1] Supplementary data for this paper are available from the IUCr electronic archives (Reference: WS5049). Services for accessing these data are described at the back of the journal.

Table 1
Experimental details.

	(I*a*)	(I*b*)	(I*c*)	(II)	(III)
Crystal data					
Chemical formula	$C_{12}H_9ClN_4O_3$	$C_{12}H_9ClN_4O_3$	$C_{12}H_9ClN_4O_3$	$C_{12}H_9ClN_4O_3$	$C_{12}H_9ClN_4O_3$
M_r	292.68	292.68	292.68	292.68	292.68
Cell setting, space group	Monoclinic, *Cc*	Monoclinic, $P2_1$	Orthorhombic, *Pbcn*	Monoclinic, $P2_1/c$	Monoclinic, *Cc*
Temperature (K)	120 (2)	120 (2)	120 (2)	120 (2)	120 (2)
a, *b*, *c* (Å)	4.8443 (2), 22.7344 (16), 11.4216 (8)	6.1515 (9), 4.7875 (5), 20.748 (3)	22.2727 (3), 8.2207 (4), 13.5916 (7)	9.0691 (3), 19.6472 (5), 7.4302 (3)	4.58110 (10), 24.8913 (13), 11.2782 (6)
β (°)	97.636 (4)	97.540 (7)	90.00	110.424 (2)	94.095 (3)
V (Å^3)	1246.73 (13)	605.75 (14)	2488.58 (18)	1240.70 (7)	1282.77 (10)
Z	4	2	8	4	4
D_x (Mg m^{-3})	1.559	1.605	1.562	1.567	1.516
Radiation type	Mo $K\alpha$	Mo $K\alpha$	Mo $K\alpha$	Mo $K\alpha$	Mo $K\alpha$
No. of reflections for cell parameters	2572	2628	2853	2846	2550
μ (mm^{-1})	0.32	0.33	0.32	0.32	0.31
Crystal form, colour	Lath, yellow	Plate, colourless	Block, colourless	Lath, orange	Plate, yellow
Crystal size (mm)	0.70 × 0.18 × 0.08	0.20 × 0.04 × 0.01	0.46 × 0.42 × 0.22	0.34 × 0.22 × 0.08	0.50 × 0.20 × 0.06
Data collection					
Diffractometer	Bruker–Nonius 95 mm CCD camera on κ goniostat	Bruker–Nonius 95 mm CCD camera on κ goniostat	Bruker–Nonius 95 mm CCD camera on κ goniostat	Bruker–Nonius 95 mm CCD camera on κ goniostat	Bruker–Nonius 95 mm CCD camera on κ goniostat
Data collection method	φ and ω scans	φ and ω scans	φ and ω scans	φ and ω scans	φ and ω scans
Absorption correction	Multi-scan	Multi-scan	Multi-scan	Multi-scan	Multi-scan
T_{min}	0.807	0.948	0.867	0.899	0.860
T_{max}	0.975	0.997	0.933	0.975	0.982
No. of measured, independent and observed reflections	5777, 2572, 2254	9293, 2628, 1322	15 916, 2853, 2293	14 751, 2846, 2179	5895, 2550, 2343
Criterion for observed reflections	$I > 2\sigma(I)$	$I > 2\sigma(I)$	$I > 2\sigma(I)$	$I > 2\sigma(I)$	$I > 2\sigma(I)$
R_{int}	0.029	0.178	0.036	0.043	0.044
θ_{max} (°)	27.5	27.5	27.5	27.5	27.5
Refinement					
Refinement on	F^2	F^2	F^2	F^2	F^2
$R[F^2 > 2\sigma(F^2)]$, $wR(F^2)$, S	0.034, 0.075, 1.06	0.074, 0.164, 0.96	0.032, 0.087, 1.04	0.038, 0.097, 1.03	0.036, 0.084, 1.05
No. of parameters	181	182	181	181	181
H-atom treatment	Constrained to parent site	Constrained to parent site	Constrained to parent site	Constrained to parent site	Constrained to parent site
Weighting scheme	$w = 1/[\sigma^2(F_o^2) + (0.0337P)^2 + 0.2325P]$, where $P = (F_o^2 + 2F_c^2)/3$	$w = 1/[\sigma^2(F_o^2) + (0.0578P)^2]$, where $P = (F_o^2 + 2F_c^2)/3$	$w = 1/[\sigma^2(F_o^2) + (0.0444P)^2 + 0.7122P]$, where $P = (F_o^2 + 2F_c^2)/3$	$w = 1/[\sigma^2(F_o^2) + (0.0408P)^2 + 0.5906P]$, where $P = (F_o^2 + 2F_c^2)/3$	$w = 1/[\sigma^2(F_o^2) + (0.0311P)^2 + 0.3107P]$, where $P = (F_o^2 + 2F_c^2)/3$
$(\Delta/\sigma)_{max}$	<0.0001	<0.0001	0.002	<0.0001	0.001
$\Delta\rho_{max}$, $\Delta\rho_{min}$ (e Å^{-3})	0.19, −0.23	0.36, −0.35	0.25, −0.33	0.30, −0.36	0.21, −0.25
Extinction method	None	*SHELXL*	None	None	None
Extinction coefficient	–	0.035 (7)	–	–	–
Absolute structure	Flack (1983), 1126 Friedel pairs	Flack (1983), 1081 Friedel pairs	–	–	Flack (1983), 1069 Friedel pairs
Flack parameter	−0.05 (5)	0.09 (16)	–	–	−0.01 (6)

Computer programs used: *COLLECT* (Hooft, 1999), *DENZO* (Otwinowski & Minor, 1997), *OSCAIL* (McArdle, 2003), *SHELXS*97 and *SHELXL*97 (Sheldrick, 1997), *PLATON* (Spek, 2003), *PRPKAPPA* (Ferguson, 1999), *SADABS* (Sheldrick, 2003).

3.2. Molecular conformations

In each of (I*a*)–(I*c*), II and (III) (Fig. 1), the two N atoms of the hydrazino moiety, N17 and N21, exhibit very shallow pyramidalization, and the torsional angle C13—C17—N17—N21 is close to 180° in each compound (Table 2): the near planarity of this central spacer unit provides a convenient reference for the conformation of the remainder of the molecule. The pyridyl ring, where the atom-numbering is defined by the location of the N and Cl atoms, makes torsional angles with the N17—C17—C13 plane ranging from less than 90° in the orthorhombic polymorph (I*c*) of compound (I) to almost 150° in polymorph (I*b*). Likewise the torsional angles about the N17—N21 bonds range from just over 70° in compound (III) to almost 150° in (I*b*).

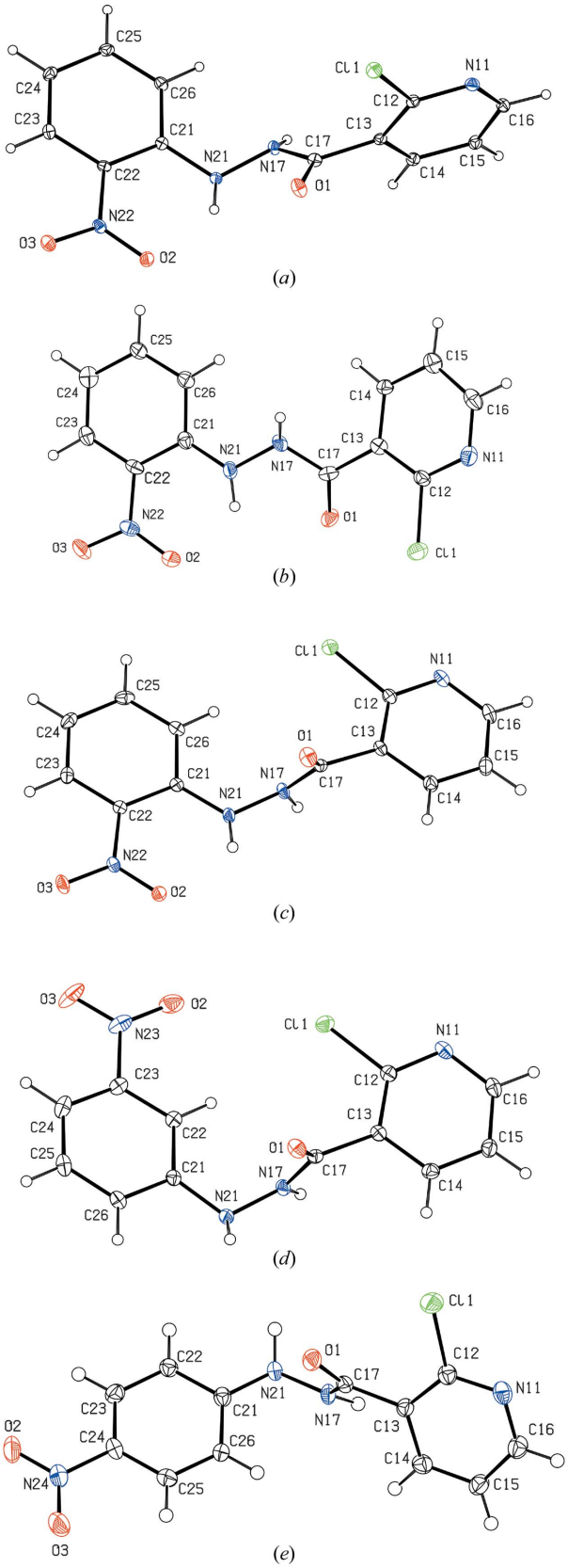

Figure 1
The molecule of (*a*) compound (I) in the *Cc* polymorph (I*a*); (*b*) compound (I) in the $P2_1$ polymorph (I*b*); (*c*) compound (I) in the *Pbcn* polymorph (I*c*); (*d*) compound (II); (*e*) compound (III), showing the atom-labelling schemes. Displacement ellipsoids are drawn at the 30% probability level.

The nitrated aryl ring, where for isomers (I) and (II) the atom-numbering is determined by the location of the nitro group, is generally nearly co-planar with the C21—N21—N17 plane: in each polymorph of compound (I), the nitro group is located such that a rather short intramolecular N21—H21···O2 contact is possible (Table 3), and this may have some influence on the conformation about the C21—N21 bond. Certainly, the presence of this contact, whether or not it is regarded as a genuine hydrogen bond, appears to preclude the participation of the N21—H21 bond in intermolecular hydrogen bonding in polymorphs (I*a*) and (I*b*), although not in polymorph (I*c*). The torsional angles show that in each compound the molecules are chiral; however, for each of (I*a*), (I*c*), (II) and (III), the space group accommodates equal numbers of the two enantiomers: in (I*b*), each crystal contains only a single enantiomer, but the absolute configuration of the molecules in the crystal selected for data collection has no chemical significance.

3.3. Supramolecular structures

3.3.1. Polymorphs of compound (I). The molecules of the *Cc* polymorph (I*a*) (Fig. 1) are linked into sheets by a combination of one N—H···O hydrogen bond and two independent C—H···O hydrogen bonds (Table 3). Each hydrogen bond acting in isolation generates a simple chain motif, and the combination of the three independent chains generates a sheet. Amido atom N17 in the molecule at (x, y, z) acts as hydrogen-bond donor to carbonyl atom O1 in the molecule at $(-1 + x, y, z)$, so generating by translation a $C(4)$ (Bernstein *et al.*, 1995) chain running parallel to the [100] direction. The atoms C16 and C25 in the molecule at (x, y, z) act as hydrogen-bond donors, respectively, to nitro atom O2 in the molecules at $(-\frac{1}{2} + x, \frac{3}{2} - y, \frac{1}{2} + z)$ and $(-1 + x, 1 - y, \frac{1}{2} + z)$, so forming, respectively, a $C(12)$ chain running parallel to the $[\bar{1}01]$ direction and generated by the *n*-glide plane at $y = 0.75$, and a $C(7)$ chain running parallel to the $[\bar{2}01]$ direction and generated by the *c*-glide plane at $y = 0.5$. The combination of these three chain motifs then generates a complex sheet parallel to (010), but there are no direction-specific interactions between adjacent sheets.

The formation of the sheet structure in the $P2_1$ monoclinic polymorph (I*b*) of compound (I) (Fig. 1*b*) is readily analysed in terms of two one-dimensional substructures. In the first of these, the amido atom N17 in the molecule at (x, y, z) acts as a hydrogen-bond donor to the carbonyl atom O1 in the molecule at $(x, 1 + y, z)$, so generating by translation a $C(4)$ chain running parallel to the [010] direction. This chain is reinforced by a C—H···O hydrogen bond where the pyridyl C16 atom at (x, y, z) acts as a donor to the pyridyl N11 atom in the molecule at $(2 - x, \frac{1}{2} + y, 1 - z)$, thereby forming a $C(3)$ chain generated by the 2_1 screw axis along $(1, y, \frac{1}{2})$. The combination of the $C(3)$ and $C(4)$ chains along [010] generates a chain of edge-fused $R_3^3(16)$ rings (Fig. 2). In the second substructure, the aryl C25 atom in the molecule at (x, y, z) acts as a hydrogen-bond donor to the nitro O3 atom in the molecule at $(1 + x, 1 + y, z)$, so generating by translation a $C(7)$ chain

Table 2
Selected torsional angles (°) for compounds (I)–(III).

Parameter	(I*a*)	(I*b*)	(I*c*)	(II)	(III)
C12—C13—C17—N17	127.1 (2)	145.7 (6)	80.38 (17)	94.63 (19)	133.8 (2)
C13—C17—N17—N21	166.29 (18)	−171.1 (5)	172.60 (12)	174.00 (13)	−175.06 (18)
C17—N17—N21—C21	123.8 (2)	−149.9 (6)	101.92 (15)	82.22 (18)	−74.0 (3)
N17—N21—C21—C22	−158.11 (18)	−179.4 (6)	179.36 (12)	16.8 (2)	168.99 (18)
C21—C22—N22—O2	−1.7 (3)	−3.4 (9)	4.56 (19)	–	–
C21—C22—N22—O3	178.28 (19)	174.7 (6)	−174.46 (12)	–	–
C22—C23—N23—O2	–	–	–	−5.9 (2)	–
C22—C23—N23—O3	–	–	–	174.33 (16)	–
C23—C24—N24—O2	–	–	–	–	0.7 (3)
C23—C24—N24—O3	–	–	–	–	−179.2 (2)

Table 3
Hydrogen-bond parameters (Å, °).

D—H···*A*	H···*A*	*D*···*A*	*D*—H···*A*
(I*a*)			
N17—H17···O1^{i}	1.90	2.737 (2)	168
N21—H21···O2	1.95	2.602 (2)	135
C16—H16···O2^{ii}	2.50	3.285 (3)	140
C25—H25···O2^{iii}	2.53	3.455 (3)	166
(I*b*)			
N17—H17···O1^{iv}	1.89	2.745 (7)	162
N21—H21···O2	2.00	2.595 (6)	124
C16—H16···N11^{v}	2.62	3.440 (9)	144
C25—H25···O3^{vi}	2.36	3.065 (8)	131
(I*c*)			
N17—H17···N11^{vii}	2.18	2.962 (2)	147
N21—H21···O2	2.04	2.603 (2)	121
N21—H21···O2^{viii}	2.17	2.965 (2)	150
C14—H14···O3^{viii}	2.42	3.332 (2)	160
C24—H24···O1^{ix}	2.51	3.377 (2)	152
C25—H25···O1^{x}	2.38	3.325 (2)	175
(II)			
N17—H17···N11^{xi}	2.23	3.068 (2)	160
N21—H21···O1^{ix}	2.15	3.003 (2)	162
C14—H14···O2^{xii}	2.47	3.371 (2)	158
(III)			
N17—H17···O1^{i}	1.94	2.799 (2)	158
N21—H21···N11^{x}	2.15	2.931 (3)	140
C16—H16···O1^{iii}	2.50	3.391 (3)	156

Symmetry codes: (i) $-1+x, y, z$; (ii) $-\frac{1}{2}+x, \frac{3}{2}-y, \frac{1}{2}+z$; (iii) $-1+x, 1-y, \frac{1}{2}+z$; (iv) $x, 1+y, z$; (v) $2-x, \frac{1}{2}+y, 1-z$; (vi) $1+x, 1+y, z$; (vii) $\frac{3}{2}-x, -\frac{1}{2}+y, z$; (viii) $1-x, y, \frac{3}{2}-z$; (ix) $1-x, 1-y, 1-z$; (x) $x, 1-y, -\frac{1}{2}+z$; (xi) $x, \frac{3}{2}-y, -\frac{1}{2}+z$; (xii) $1+x, y, z$.

running parallel to the [110] direction. The combination of the [010] and [110] chains generates a (001) sheet: there are no direction-specific interactions between adjacent sheets.

The supramolecular structure of the orthorhombic polymorph (I*c*) of compound (I) (Fig. 1*c*) is three-dimensional and it contains N—H···N and N—H···O hydrogen bonds, and three distinct C—H···O hydrogen bonds (Table 3), as well as an aromatic $\pi\cdots\pi$ stacking interaction. The hard hydrogen bonds with N—H donors generate two simple substructures, whose combination generates sheets which are linked into a three-dimensional framework structure by two motifs constructed from C—H···O hydrogen bonds. The hydrazino N17 atom in the molecule at (x, y, z) acts as a hydrogen-bond donor to the pyridyl N11 atom in the molecule at $(\frac{3}{2}-x, -\frac{1}{2}+y, z)$, so forming a $C(6)$ chain running parallel to the [010] direction and generated by the *b*-glide plane at $x = 0.75$. In a more complex substructure, albeit of finite zero-dimensional character, the hydrazino N21 atom in the molecule at (x, y, z) acts as a hydrogen-bond donor to the nitro O2 atom in the molecule at $(1-x, y, \frac{3}{2}-z)$, thereby producing a cyclic $R_2^2(12)$ dimer generated by the twofold rotation axis along $(\frac{1}{2}, y, \frac{3}{4})$ (Fig. 3). This dimer is reinforced by paired C—H···O hydrogen bonds generating a $R_2^2(20)$ ring concentric with the $R_2^2(12)$ ring. When the intramolecular hydrogen bond is taken into account, this dimeric aggregate contains a total of five edge-fused hydrogen-bonded rings in a cruciform array (Fig. 3). The two molecules in this aggregate form parts of the $C(6)$ chains generated, respectively, by glide planes at $x = 0.75$ and $x = 0.25$, and hence the propagation by the space group of the two motifs generates a deeply puckered (001) sheet: if just the N—H···N and intermolecular N—H···O hydrogen bonds are considered, the sheet contains alternating $R_2^2(12)$ and $R_6^6(40)$ rings (Fig. 4); if the other hydrogen bonds within the dimers are also considered, the sheet description becomes much more complex.

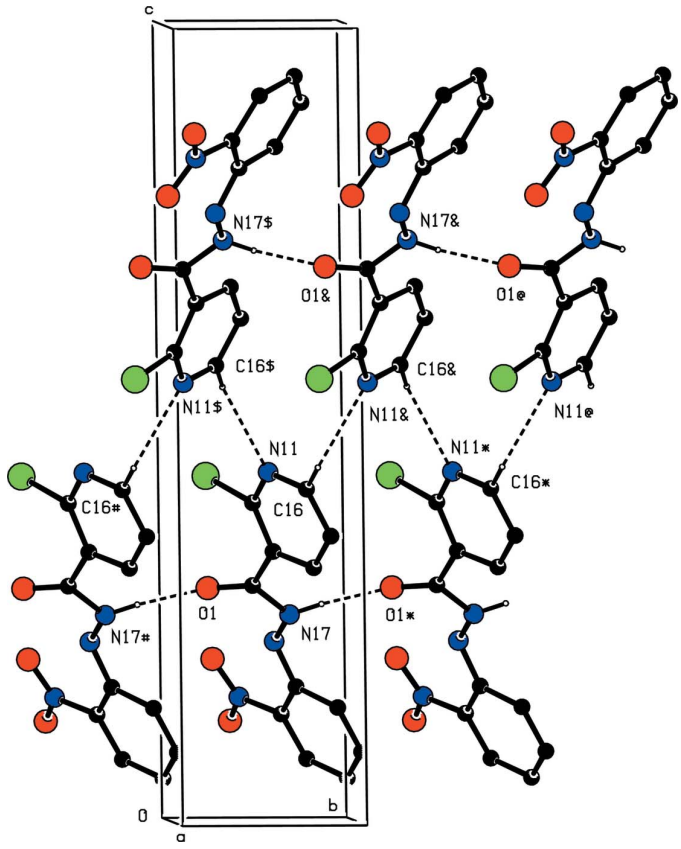

Figure 2
Part of the crystal structure of the $P2_1$ polymorph (I*b*) showing the formation of a chain of edge-fused rings along [010]. For the sake of clarity the H atoms not involved in the motifs shown have been omitted. The atoms marked with an asterisk (*), a hash (#), a dollar sign ($), an ampersand (&) or an 'at' sign (@) are at the symmetry positions $(x, 1+y, z)$, $(x, -1+y, z)$, $(2-x, -\frac{1}{2}+y, 1-z)$, $(2-x, \frac{1}{2}+y, 1-z)$ and $(2-x, \frac{3}{2}+y, 1-z)$, respectively.

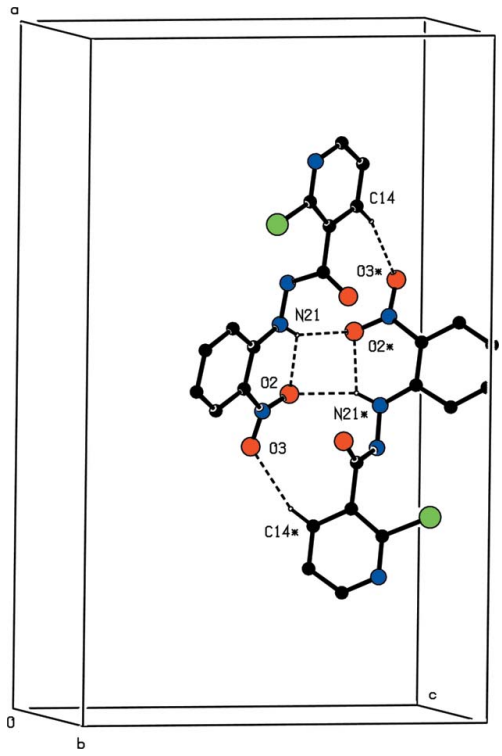

Figure 3
Part of the crystal structure of the orthorhombic polymorph (I*c*) showing the formation of a dimeric aggregate containing five hydrogen-bonded rings. For the sake of clarity the H atoms not involved in the motifs shown have been omitted. The atoms marked with an asterisk (*) are at the symmetry position $(1 - x, y, \frac{3}{2} - z)$.

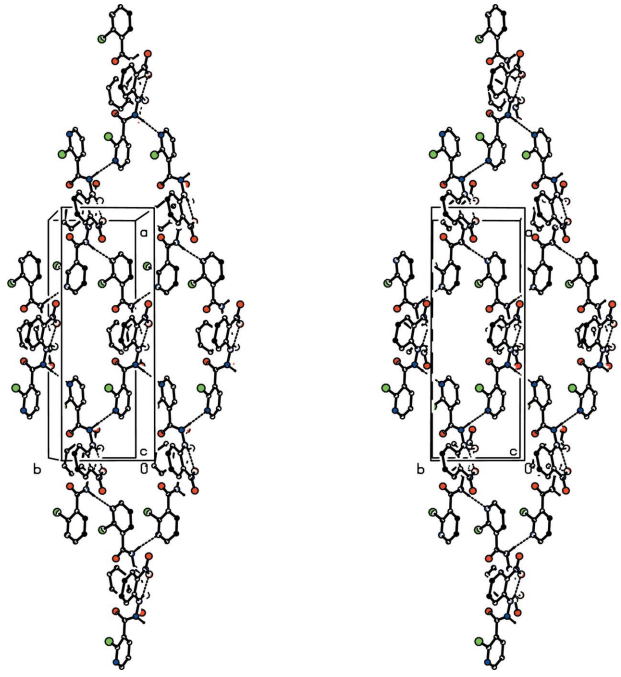

Figure 4
Stereoview of part of the crystal structure of the orthorhombic polymorph (I*c*) showing the formation of a (001) sheet. For the sake of clarity the H atoms not involved in the motifs shown have been omitted, and only the N—H···N and the intermolecular N—H···O hydrogen bonds are shown.

Adjacent (001) sheets are linked by two different motifs involving two different C—H···O hydrogen bonds. In the first of these, the aryl C24 atom in the molecule at (x, y, z) acts as a hydrogen-bond donor to the carbonyl O1 atom in the molecule at $(1 - x, 1 - y, 1 - z)$, so generating a centrosymmetric $R_2^2(18)$ ring, where the two molecular components lie, respectively, in the (001) sheets generated by the twofold axes at $y = 0.75$ and $y = 0.25$. In the second such motif, the aryl C25 atom in the molecule at (x, y, z) acts as a hydrogen-bond donor to the carbonyl O1 atom in the molecule at $(x, 1 - y, -\frac{1}{2} + z)$, so forming a $C(8)$ chain running parallel to the [001] direction and generated by the *c*-glide plane at $y = \frac{1}{2}$.

3.3.2. Compound (II). The molecules of compound (II) (Fig. 1*d*) are linked into a three-dimensional framework structure by a combination of three hydrogen bonds, one each of N—H···O, N—H···N and C—H···O types (Table 2), weakly augmented by a $\pi\cdots\pi$ stacking interaction. The formation of the framework is readily analysed in terms of simple substructures in zero, one and two dimensions. The basic building block in the structure can be regarded as a cyclic centrosymmetric dimer generated by paired N—H···O hydrogen bonds. The N21 atom in the molecule at (x, y, z) acts as a hydrogen-bond donor to the O1 atom in the molecule at $(1 - x, 1 - y, 1 - z)$, thereby generating by inversion a centrosymmetric $R_2^2(10)$ dimer centred at $(\frac{1}{2}, \frac{1}{2}, \frac{1}{2})$. Dimers of this type are linked into two further substructures, one of which is one-dimensional and the other two-dimensional, and each is generated by the action of just one additional hydrogen bond.

The $R_2^2(10)$ dimers are linked into a chain of edge-fused rings by means of the C—H···O hydrogen bond. The pyridyl C14 atom in the molecule at (x, y, z) acts as a hydrogen-bond donor to the nitro O2 atom in the molecule at $(1 + x, y, z)$, and propagation of this hydrogen bond by translation and inversion links the $R_2^2(10)$ units into a chain of edge-fused rings running parallel to the [100] direction, with $R_2^2(10)$ rings centred at $(n + \frac{1}{2}, \frac{1}{2}, \frac{1}{2})$ (n = zero or integer) and $R_4^4(24)$ rings centred at $(n, \frac{1}{2}, \frac{1}{2})$ (n = zero or integer) (Fig. 5).

In the second mode of linkage of the $R_2^2(10)$ dimers, the N—H···N hydrogen bond links these dimers into the two-dimensional substructure. The N17 atoms in the molecules at (x, y, z) and $(1 - x, 1 - y, 1 - z)$, which make up the dimer centred at $(\frac{1}{2}, \frac{1}{2}, \frac{1}{2})$, act as hydrogen-bond donors, respectively, to the ring N11 atoms in the molecules at $(x, \frac{3}{2} - y, -\frac{1}{2} + z)$ and $(1 - x, -\frac{1}{2} + y, \frac{3}{2} - z)$, which lie in the dimers centred at $(\frac{1}{2}, 1, 0)$ and $(\frac{1}{2}, 0, 1)$, respectively. Similarly, the ring N11 atoms in the molecules at (x, y, z) and $(1 - x, 1 - y, 1 - z)$ accept hydrogen bonds from the atoms N17 in the molecules at $(x, \frac{3}{2} - y, \frac{1}{2} + z)$ and $(1 - x, -\frac{1}{2} + y, \frac{1}{2} - z)$, respectively, which themselves lie in the dimers centred at $(\frac{1}{2}, 1, 1)$ and $(\frac{1}{2}, 0, 0)$, respectively. Propagation of these two hydrogen bonds then generates a (100) sheet of alternating $R_2^2(10)$ and $R_6^6(30)$ rings, both of which are centrosymmetric (Fig. 6).

The combination of the [100] chain (Fig. 5) and the (100) sheet (Fig. 6) is sufficient to define the entire three-dimen-

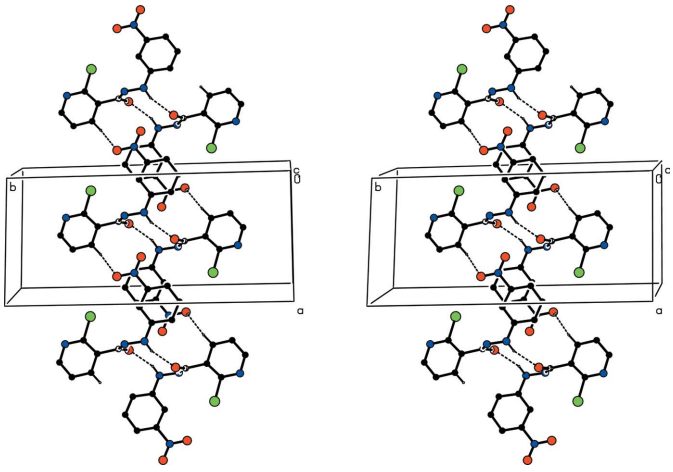

Figure 5
Stereoview of part of the crystal structure of isomer (II) showing the formation of a [100] chain of edge-fused $R_2^2(10)$ and $R_4^4(24)$ rings. For the sake of clarity the H atoms not involved in the motif shown have been omitted.

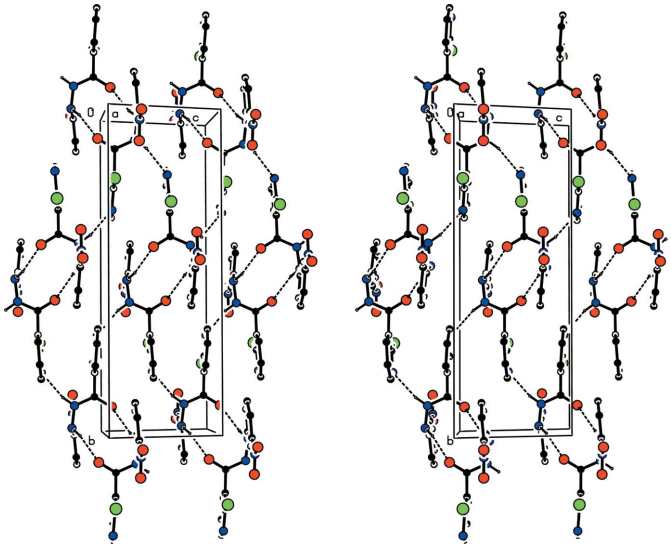

Figure 6
Stereoview of part of the crystal structure of isomer (II) showing the formation of a (100) sheet of $R_2^2(10)$ and $R_6^6(30)$ rings. For the sake of clarity the H atoms bonded to C atoms have been omitted.

sional framework structure. The framework is weakly augmented by a $\pi\cdots\pi$ stacking interaction between the nitrophenyl ring in the molecule at (x, y, z) and the corresponding rings in the molecules at both ($x, \frac{3}{2} - y, \frac{1}{2} + z$) and ($x, \frac{3}{2} - y, -\frac{1}{2} + z$); adjacent rings are inclined to one another by 8.6 (2)°, with a ring–centroid separation of 3.737 (20) Å and an interplanar spacing of *ca* 3.42 Å, corresponding to a ring offset of *ca* 1.51 Å. In this manner a π-stacked chain along [001] is generated by the *c*-glide plane at $y = 0.75$.

3.3.3. Compound (III). The molecules of (III) (Fig. 1*e*) are linked into sheets by a combination of N—H···O, N—H···N and C—H···O hydrogen bonds (Table 3), and the formation of these sheets is conveniently analysed in terms of three

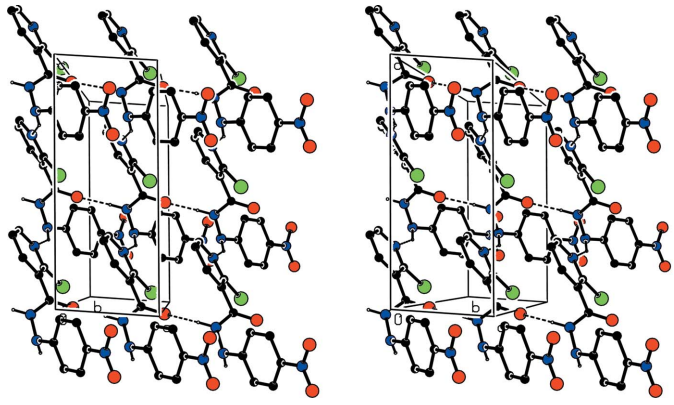

Figure 7
Stereoview of part of the crystal structure of isomer (III), showing the formation of a (010) sheet of $R_4^4(20)$ rings. For the sake of clarity the H atoms not involved in the motif shown have been omitted.

independent one-dimensional substructural motifs, each formed by just one type of hydrogen bond.

The N17 atom in the molecule at (x, y, z) acts as a hydrogen-bond donor to atom O1 in the molecule at ($-1 + x$, y, z) so generating by translation a $C(4)$ chain running parallel to the [100] direction. By contrast, the N21 atom at (x, y, z) acts as a donor to the ring N11 atom in the molecule at (x, $1 - y$, $-\frac{1}{2} + z$), so forming a $C(7)$ chain running parallel to the [001] direction and generated by the *c*-glide plane at $y = 0.5$. The combination of these two motifs built from hard hydrogen bonds generates a (010) sheet in the form of a (4,4) net (Batten & Robson, 1998) built from a single type of $R_4^4(20)$ ring (Fig. 7). This sheet is modestly reinforced by the third one-dimensional motif: the C16 atom in the heterocyclic ring at (x, y, z) acts as a hydrogen-bond donor to the carbonyl O1 atom in the molecule at ($-1 + x$, $1 - y$, $\frac{1}{2} + z$), so forming a $C(7)$ chain running parallel to the [$\bar{2}$01] direction and lying wholly within the reference (010) sheet.

Two (010) sheets pass through each unit cell, in the domains $0.17 < y < 0.83$ and $0.67 < y < 1.33$, but there are no direction-specific interactions between adjacent sheets: in particular C—H···π(arene) hydrogen bonds and aromatic $\pi\cdots\pi$ stacking interactions are both absent from the structure of (III).

3.4. General discussion of the structures

The three polymorphs of isomer (I) were obtained by crystallization from three different solvents: ethanol for polymorph (I*a*), 1,2-dichloroethane for polymorph (I*b*) and acetone for polymorph (I*c*). We have obtained no evidence for any concomitant polymorphism (Bernstein *et al.*, 1999) in this series.

It is striking that polymorph (I*b*) has a density significantly higher than those of polymorphs (I*a*) and (I*c*), which are almost identical (Table 1). If it is assumed that the polymorph of highest density is the thermodynamically most stable form (Burger & Ramsberger, 1979), then it is surprising that this polymorph, (I*b*), was actually obtained before either (I*a*) or (I*c*), as the formation of the most stable polymorph sometimes

precludes the subsequent preparation of the less stable forms (Dunitz & Bernstein, 1995). In the event, the crystals of polymorphs (I*a*) and (I*c*) appear to be indefinitely stable when kept in the same laboratory environment as polymorph (I*b*). However, it may be noted that there are no simple relationships between the unit-cell dimensions of these three polymorphs, so that simple displacive phase transformations between polymorphs (I*a*)–(I*c*) may not be possible.

In no two of the polymorphs (I*a*)–(I*c*) are the same selection of direction-specific intermolecular interactions utilized in the construction of the supramolecular structures. Thus, the two-dimensional supramolecular structure of polymorph (I*a*) contains N—H···O and C—H···O hydrogen bonds, while that of (I*b*) utilizes a C—H···N hydrogen bond in addition: polymorph (I*c*) utilizes N—H···O, N—H···N and C—H···O hydrogen bonds, as well as a $\pi\cdots\pi$ stacking interaction in the formation of its three-dimensional supramolecular structure. The same types of hydrogen bonds as found in the structure of polymorph (I*c*) are also found in the structures of isomers (II) and (III), but the supramolecular structures of these isomers are, respectively, three-dimensional and two-dimensional.

It is of interest to compare here the supramolecular structures of the hydrazides (I)–(III) with those of the corresponding amides (IV)–(VI), respectively (de Souza *et al.*, 2005). In the 2-nitro isomer of the amide series, compound (IV), the sole N—H···O hydrogen bond is intramolecular rather than intermolecular, whereas in each polymorph of the analogous hydrazide (I) there are both intramolecular and intermolecular N—H···O hydrogen bonds: instead, the molecules of compound (IV) are linked by two C—H···O hydrogen bonds to form chains of edge-fused $R_2^2(14)$ and $R_4^4(24)$ rings. Hence, the supramolecular structure of (IV) is one-dimensional, as compared with the two-dimensional structures of polymorphs (I*a*) and (I*b*) and the three-dimensional structure of polymorph (I*c*), and this difference may be traced directly to the additional amino —NH— unit in the hydrazide (I) as compared with the amide (IV). The 3-nitro amide, compound (V), crystallizes as a monohydrate and the structure contains intermolecular hydrogen bonds of N—H···O, O—H···O and O—H···N types. However, despite the profusion of strong hydrogen bonds, the supramolecular structure of (V) is again only one-dimensional in the form of a chain containing two types of $R_4^4(16)$ ring, whereas the supramolecular structure of the analogous hydrazide (II) is three-dimensional, despite the absence of both O—H···O and O—H···N hydrogen bonds. Finally, the 4-nitro amide, compound (VI), is the only member of the amide series (IV)–(VI) to exhibit the formation of N—H···N hydrogen bonds, despite the presence of such hydrogen bonds in each of the hydrazides (I*c*), (II) and (III), although they are absent from the structures of (I*a*) and (I*b*). Compound (VI) crystallizes with $Z' = 2$, and the molecules are linked by two independent N—H···N hydrogen bonds to form simple $C_2^2(12)$ chains. Thus, in each of the amides (IV)–(VI) the supramolecular structure is one-dimensional in contrast to the structures of the hydrazides (I)–(III), whose structure are all two- or three-dimensional.

4. Concluding discussion

Such is the variation in supramolecular aggregation within the series of closely related compounds (I)–(VI) that it would be impossible to predict the supramolecular characteristics of any one compound from a detailed knowledge of all the others, in respect not only of the overall supramolecular structure or even its dimensionality but also of the range of direction-specific intermolecular interactions which are present. To this extent, the behaviour of (I)–(VI) reflects that of other series of closely related compounds which we have recently studied, in which small geometric changes, such as the location of a single common substituent, often induce marked but unpredictable changes in the pattern of supramolecular aggregation (Ferguson *et al.*, 2005; Glidewell *et al.*, 2002, 2005, 2006; Kelly *et al.*, 2002; Wardell *et al.*, 2002; Wardell, Low *et al.*, 2006). The underlying structural systematics, which depend upon the subtle interplay of weak intermolecular forces and low intramolecular rotational barriers, do not yet seem to be amenable to either heuristic or computational analysis.

In recent studies of the variations both in the patterns of supramolecular aggregation and, in particular, in the range of direction-specific intermolecular interactions present, in series of isomeric compounds we have observed several instances where one or more of the isomers within a particular series exhibits polymorphism, usually solvent-dependent polymorphism. For example, three of the nine isomeric nitrobenzylidene-iodoanilines (Glidewell *et al.*, 2002) have been found (Ferguson *et al.*, 2005) to exhibit solvent-dependent polymorphism: of the 11 structural forms so far characterized, no two utilize the same array of direction-specific intermolecular interactions in their supramolecular structures. Similarly, one of the isomers of 2-(nitrophenylaminocarbonyl)benzoic acid exhibits solvent-dependent polymorphism and, again, no two of the supramolecular structures in this series utilize the same combination of direction-specific intermolecular interactions (Glidewell *et al.*, 2004). Finally, one of the six isomers of 1,4-bis(nitrophenyl)2,3-diaza-1,3-butadiene exhibits dimorphism with different intermolecular interactions manifested in the two forms (Glidewell *et al.*, 2006). As we have noted previously (Glidewell *et al.*, 2002), such structural variations across simple series of geometric isomers, allied to the occurrence of polymorphism, as in the present series of compounds (I)–(III), presents a keen test for computational attempts at the *ab initio* prediction of the crystal structures of molecular compounds, an endeavour where convincing success remains tantalisingly elusive (Lommerse *et al.*, 2000; Motherwell *et al.*, 2002; Day *et al.*, 2005).

Equally testing in terms of structure prediction are a number of the areas noted in this paper:

(i) the differences in supramolecular structures between corresponding members of closely related series of compounds, as in the hydrazides (I)–(III) *versus* the respective amides (IV)–(VI) as discussed above (§3.4);

(ii) the differences within such series not only between the types of hydrogen bond present but also between their

detailed actions: for example, in the series (I)–(III) described here the atoms N17 form intermolecular N—H···O hydrogen bonds in each of (I*a*), (I*b*) and (III), but intermolecular N—H···N hydrogen bonds in (I*c*) and (II), while the atoms N21 form intramolecular hydrogen bonds in (I*a*) and (I*b*), a three-centre N—H···$(O)_2$ system involving both intramolecular and intermolecular components in (I*c*), an intermolecular N—H···O hydrogen bond in (II) and an intermolecular N—H···N hydrogen bond in (III); and finally

(iii) the question of whether pairs of analogous compounds containing, for example, a methyl substituent *versus* a chloro substituent, or a chloro substituent *versus* a bromo substituent, are or are not isomorphous and isostructural. All of these areas present challenges for future work.

The difficulty of structure prediction appears to be a characteristic of the crystal structures of molecular compounds where all of the intermolecular forces are comparatively weak but of comparable magnitudes to the rotational energy barriers associated with single bonds, so that the molecular conformations are direct reflections of the intermolecular interactions. For this reason alone, molecular conformations computed for isolated molecules are unlikely ever to reproduce the conformations observed experimentally in the crystalline state. Compounds whose molecules contain internal degrees of freedom such as rotations about single bonds, particularly where aryl rings are connected to a semi-rigid unit, as in the examples discussed here, seem to pose particular difficulty in attempts at structure prediction, possibly associated with the delicate interplay of intramolecular and intermolecular forces.

X-ray data for compounds (I)–(III) were collected at the EPSRC X-ray Crystallographic Service, University of Southampton, UK: the authors thank the staff of the Service for all their help and advice. JLW and SMSVW thank CNPq and FAPERJ for financial support.

References

Allen, F. H. (2002). *Acta Cryst.* B**58**, 380–388.
Batten, S. R. & Robson, R. (1998). *Angew. Chem. Int. Ed.* **37**, 1460–1494.
Baur, W. H. & Kassner, D. (1992). *Acta Cryst.* B**48**, 356–369.
Bernstein, J., Davey, R. J. & Henck, J.-O. (1999). *Angew. Chem. Int. Ed.* **38**, 3440–3461.
Bernstein, J., Davis, R. E., Shimoni, L. & Chang, N.-L. (1995). *Angew. Chem. Int. Ed. Engl.* **34**, 1555–1573.
Burger, A. & Ramsberger, R. (1979). *Mikrochim. Acta*, **2**, 259–271.
Cuffini, S., Glidewell, C., Low, J. N., de Oliveira, A. G., de Souza, M. V. N., Vasconcelos, T. R. A., Wardell, S. M. S. V. & Wardell, J. L. (2006). *Acta Cryst.* B**62**, 651–665.
Day, G. M. *et al.* (2005). *Acta Cryst.* B**61**, 511–527.
Dunitz, J. D. & Bernstein, J. (1995). *Acc. Chem. Res.* **28**, 193–200.
Ferguson, G. (1999). *PRPKAPPA*. University of Guelph, Canada.
Ferguson, G., Glidewell, C., Low, J. N., Skakle, J. M. S. & Wardell, J. L. (2005). *Acta Cryst.* C**61**, o445–o449.
Flack, H. D. (1983). *Acta Cryst.* A**39**, 876–881.
Glidewell, C., Howie, R. A., Low, J. N., Skakle, J. M. S., Wardell, S. M. S. V. & Wardell, J. L. (2002). *Acta Cryst.* B**58**, 864–876.
Glidewell, C., Low, J. N., Skakle, J. M. S. & Wardell, J. L. (2004). *Acta Cryst.* C**60**, o120–o124.
Glidewell, C., Low, J. N., Skakle, J. M. S. & Wardell, J. L. (2005). *Acta Cryst.* C**61**, o312–o316.
Glidewell, C., Low, J. N., Skakle, J. M. S. & Wardell, J. L. (2006). *Acta Cryst.* B**62**, 666–675.
Hooft, R. W. W. (1999). *Collect.* Nonius BV, Delft, The Netherlands.
Kelly, C. J., Skakle, J. M. S., Wardell, J. L., Wardell, S. M. S. V., Low, J. N. & Glidewell, C. (2002). *Acta Cryst.* B**58**, 94–108.
Lommerse, J. P. M., Motherwell, W. D. S., Ammon, H. L., Dunitz, J. D., Gavezzotti, A., Hofmann, D. W. M., Leusen, F. J. J., Mooij, W. T. M., Price, S. L., Schweizer, B., Schmidt, M. U., van Eijck, B. P., Verwer, P. & Williams, D. E. (2000). *Acta Cryst.* B**56**, 697–714.
McArdle, P. (2003). *OSCAIL for Windows.* Version 10. Crystallography Centre, Chemistry Department, NUI Galway, Ireland.
Marsh, R. E. (1997). *Acta Cryst.* B**53**, 317–322.
Marsh, R. E. (2004). *Acta Cryst.* B**60**, 252–253.
Motherwell, W. D. S. *et al.* (2002). *Acta Cryst.* B**58**, 647–761.
Otwinowski, Z. & Minor, W (1997). *Methods in Enzymology*, Vol. 276, *Macromolecular Crystallography*, Part A, edited by C. W. Carter Jr & R. M. Sweet, pp. 307–326. New York: Academic Press.
Sheldrick, G. M. (1997). *SHELXS*97 and *SHELXL*97. University of Göttingen, Germany.
Sheldrick, G. M. (2003). *SADABS.* Version 2.10. University of Göttingen, Germany.
Souza, M. V. N. de, Vasconcelos, T. R. A., Wardell, S. M. S. V., Wardell, J. L., Low, J. N. & Glidewell, C. (2005). *Acta Cryst.* C**61**, o204–o208.
Spek, A. L. (2003). *J. Appl. Cryst.* **36**, 7–13.
Wardell, J. L., Low, J. N., Skakle, J. M. S. & Glidewell, C. (2006). *Acta Cryst.* B**62**, 931–943.
Wardell, J. L., Wardell, S. M. S. V., Skakle, J. M. S., Low, J. N. & Glidewell, C. (2002). *Acta Cryst.* C**58**, o428–o430.
Wardell, S. M. S. V., Wardell, J. L., Low, J. N. & Glidewell, C. (2006). *Acta Cryst.* C**62**, o170–o172.
Wilson, A. J. C. (1976). *Acta Cryst.* A**32**, 994–996.